International Journal of Thermophysics, Vol. 25, No. 5, September 2004 (© 2004)

Thermal Characterization of Agar Encapsulated in TiO_2 Sol–Gel[1]

T. López,[2] M. Picquart,[2] G. Aguirre,[2] G. Arriola,[2] Y. Freile,[3] D. H. Aguilar,[3] P. Quintana,[3,4] J. J. Alvarado-Gil,[3] and F. M. Vargas-Luna[5]

Thermal effusivity evolution as a function of time, of aqueous emulsions of agar encapsulated in a TiO_2 matrix synthesized by the sol–gel method, was monitored during dehydration at ambient conditions. Measurements of thermal effusivity were performed by the photoacoustic technique using a conventional cell. The results show sigmoidal growth as a function of time during the dehydration process. The data analysis shows two dehydration stages; in the first one, samples prepared at pH 7.5 show a lower dehydration time than samples prepared at pH 7. But, when the dehydration process continues, it is slowed down in the sample prepared at pH 7.5. FT-IR absorption and Raman spectroscopy are used to verify the strong interaction between the TiO_2 matrix and the agar.

KEY WORDS: agar; photoacoustic technique; Raman spectroscopy; sol–gel titania; thermal effusivity.

1. INTRODUCTION

Encapsulation of biomaterials inside sol–gel ceramic matrices has received great attention in an effort to provide a media for storing living microorganisms. However, these microorganisms must have a friendly environment in order to survive. One of the most interesting approaches is the use of agar as the host material.

[1]Paper presented at the Fifteenth Symposium on Thermophysical Properties, June 22–27, 2003, Boulder, Colorado, U.S.A.

[2]Universidad Autónoma Metropolitana-Iztapalapa, A.P. 55-534 México, D.F., 09340.
[3]Centro de Investigación y de Estudios Avanzados del IPN-Mérida, A.P. 73 Cordemex, C.P. 97310, Mérida, Yucatán, México.
[4]To whom correspondence should be addressed. E-mail: pquint@mda.cinvestav.mx
[5]Instituto de Física, Universidad de Guanajuato, León, Gto. México.

0195-928X/04/0900-1483/0

Agar comprises a family of cell-wall lipopolysaccharides extracted from marine algae (Rhodophyte), and is a hydrophilic substance that has been extensively used as a gellification agent in food and in other applications in microbiology, biochemistry, and biomolecular biology. The ability to form reversible gels simply by cooling hot aqueous solutions is the most important property of agar and can be regarded as the prototype and model for all gelling systems. On the other hand, the sol–gel method offers new possibilities for incorporating biologically active agents within ceramic xerogels at room temperature [1–5]. Sol-gel encapsulation improves the stability of the biomaterial and favors the interactions between the immobilized bio-system and the substrate. Furthermore, the sol–gel method offers many advantages due to its easy preparation characteristics, such as a constant pH level, low temperature, pore size control, etc. [6, 7]

The encapsulated biomaterials present a combination of properties of the biological and inorganic elements that can lead to new technological applications. For example, sol–gel titania is a well known photocatalyst that has been used in several environmental applications, because its efficiency promotes reactions leading to the partial or total destruction of organic pollutants. If titania is used to encapsulate a biological component, like microorganisms or agar, this biomaterial can have the ability to degrade additional biological compounds, or to improve the photodegradation properties of titania [8].

Determination of thermal properties is a useful tool in the study of materials and processes. In the last 25 years, photoacoustic (PA) techniques have proven to be valuable methods for thermal characterization of a wide range of solids [9]. The versatility of these techniques is based on the fact that they look directly at the heat generated in a sample, due to nonradiative de-excitation processes, following the absorption of the modulated light that impinges upon the sample. In particular, the microphone PA techniques are based on sound generation produced by pressure changes in the PA gas chamber due to modulated heating.

PA techniques have been widely used in the determination of thermal properties in liquids [10, 11]. Recently it has been shown that the restriction of optical transparency can be surpassed, if a variant of the conventional PA cell is used. In this case, the thermal effusivity can be determined for all kind of liquids [10].

In this paper the thermal characterization of a material composed of encapsulated agar in titania sol–gel matrix is performed. The dehydration process can be followed by monitoring the thermal effusivity as a function of time, and the process obeys a second-order kinetics. A fit of the experimental results provides the characteristic time and velocity of these

processes. The structure of encapsulated agar is studied by FT-Raman spectroscopy and FT-IR.

2. MEASUREMENTS

2.1. Sol–Gel Method

In order to prepare the titania matrix mixed with agar by the sol–gel method, a solution of agar, extracted from the red algae *Gracilarea cornea*, [12] was first prepared using 4 g of agar diluted into 40 mL of distilled water. Sol–gel titania was produced mixing titanium (IV) *n*-butoxide (Strem Chemicals 98%) and distilled water in a 1:8 relationship. The mixture was maintained with low stirring at room temperature (27°C), with a pH level of 7. Next, a 20 mL of agar solution was added drop wise and the mixture was aged for 22 h until gellation. To prepare a sample with a pH of 7.5, 1 mL of ammonium hydroxide (Baker 28%) was added before the agar solution. After the gel was formed, it was dried in a rotary evaporator system (Eseve D402-2) at ambient temperature, eliminating water and alcoxide residues.

2.2. PA Measurements

PA monitoring was carried out using the PA cell shown in Fig. 1. In this configuration the PA cell is closed, at the bottom end, by a glass window (d) and at the top end, by a removable reference substrate (c). An electret microphone (f) is used, coupled to the cavity wall, to sense the pressure fluctuations in the PA chamber produced by the periodic heating of the substrate, due to the pumping beam (e). The sample to be studied (a) is deposited inside a 1 mm high acrylic ring (b) on the external surface of the reference material (c).

The pumping light beam is produced by a He–Ne 25 mW laser, which is mechanically modulated by an optical chopper (SR540) at constant frequency ($f = 7$ Hz), for all experiments, and focused onto the reference material. The microphone signal is fed into a lock-in amplifier (SR830), from where the output signal amplitude is recorded as a function of time with a personal computer. All measurements were performed using an aluminum foil of 50 μm thickness as the reference material, with a thermal diffusivity of $0.9\,cm^2 \cdot s^{-1}$

According to the Rosencwaig and Gersho model [9], the PA signal is determined by the temperature fluctuation (θ) at the air–substrate interface. Solving the thermal diffusion equations for this configuration, this temperature can be determined. The quotient between the PA signal with

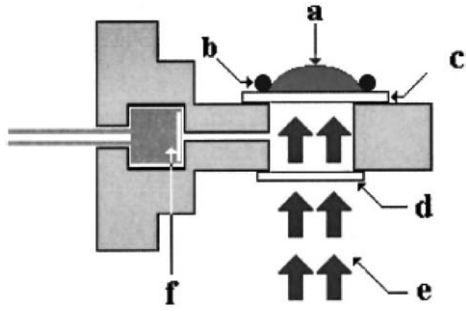

Fig. 1. Cross, section of the photoacoustic cell: (a) sample, (b) 1 mm acrylic ring, (c) aluminum reference material, (d) quartz window, (e) modulated light, and (f) microphone.

sample (θ) and without sample (θ_0) is given by [10]

$$q = \left|\frac{\theta}{\theta_0}\right| = \frac{\sqrt{\cosh(2al) - \cos(2al)}}{\sqrt{\cosh(2al) + \cos(2al)}} \times \frac{\sqrt{(b+1)^2 e^{2al} + (b-1)^2 e^{-2al} - 2(b^2-1)\cos(2al)}}{\sqrt{(b+1)^2 e^{2al} + (b-1)^2 e^{-2al} + 2(b^2-1)\cos(2al)}}. \quad (1)$$

Here, $a = (\pi f/\alpha)^{1/2}$, f is the modulation frequency of the incident light, α and l are the thermal diffusivity and thickness of the reference material, respectively; $b = \varepsilon_b/\varepsilon$ is the thermal coupling coefficient, and ε and ε_b are the thermal effusivities of the substrate and sample, respectively. It is assumed that the thermal effusivity of air is much smaller than the thermal effusivity of the substrate, which is optically opaque. Solving Eq. (1) for the thermal coupling coefficient, the thermal effusivity of the emulsion can be obtained as a function of time.

The samples to be studied were prepared mixing 2:1 (wt) of water and powdered sample. The mixture was homogenized for 30 min in an ultrasonic bath, and an emulsion was obtained. This was deposited on the 1 mm acrylic ring, which is on top of the PA chamber, as shown in Fig. 1. All experiments were performed at room temperature.

Raman spectroscopy was performed on a 910 Nicolet FT-Raman spectrometer with a power of 6 mW at the laser head; 100 scans of each sample were performed and accumulated at room temperature.

FT-IR absorption spectra were recorded at room temperature on a Perkin Elmer 1600 spectrometer equipped with a globar source and a TGS detector. Pellets were made with a mixture of 10% of agar or agar–TiO_2 and 90% of KBr.

3. RESULTS AND DISCUSSION

In Fig. 2, the photoacoustic signal (proportional to θ) normalized to its maximum value as a function of time for three different samples is shown: fresh titania xerogel and titania–agar samples with pH values of 7 and 7.5.

The results of the photoacoustic signal will be analyzed using double sigmoidal fitting functions, each of them having the following form: [10]

$$S = S_{\mathrm{m}} + \frac{S_0}{1 + \mathrm{e}^{(t-t_0)/\Delta t}} + \frac{S_p}{1 + \mathrm{e}^{(t-t_{0p})/\Delta t_p}} \tag{2}$$

where t is the time, S_{m} is the maximum value of the growth, S_0 and S_p are factors that define the value of each sigmoidal at the beginning of the process, t_0 and t_{0_p} are the time intervals when each sigmoidal process reaches its maximum derivative, and Δt and Δt_p are the mean times in which each sigmoidal growth process occurs. The results are shown in Table I. The behavior of the material is strongly affected by the presence of agar. The

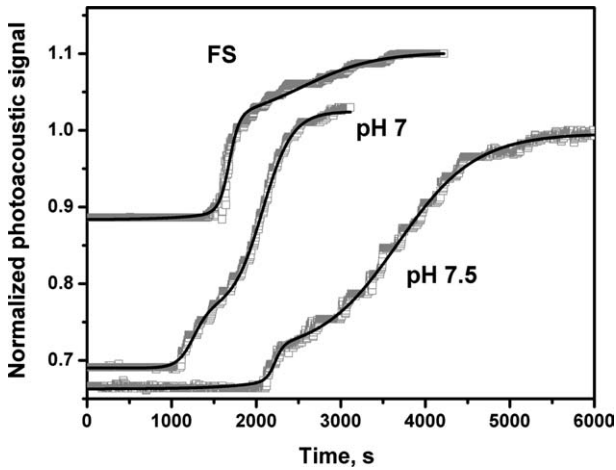

Fig. 2. Normalized photoacoustic signal as a function of time for different pH values. Continuous lines correspond to the double sigmoidal fits of the experimental data.

Table I. Characteristic Time Intervals and Initial Thermal Effusivity for the Different Samples

Sample	t_0(s)	t_{0p}(s)	Δt(s)	Δt_p(s)	ε_b(W·s$^{1/2}$·cm^{-2}·K^{-1})
Titania xerogel	1681	2538	60	437	0.085
Agar–titania pH = 7	1258	2073	94	176	0.095
Agar–titania pH = 7.5	2222	3675	51	462	0.095

characteristic times for the first (t_0) and second (t_{0p}) sigmoidal processes, are reduced at pH 7 and increased for pH 7.5, respectively, with respect to fresh titania xerogel. On the other hand, settle-down time intervals for the first (Δt) and second (Δt_p) sigmoidal processes, are similar in fresh titania and in the sample at pH 7.5.

The double sigmoidal behavior is a consequence of two different dehydration processes. The first would be related to water not strongly bonded chemically within the structure of the xerogel, and the second part of the dehydration process would imply a behavior related to the hydrophilicity of the material. These could help us to understand the delayed evaporation process for samples of pH 7.5.

Using Eq. (1), the thermal effusivity of the samples as a function of time can be determined. In Table I, the initial thermal effusivity is shown. In Fig. 3, the thermal effusivity of the same samples can be observed; for all of them the behavior exhibiting two bumps is present; however, the behavior is more pronounced for the fresh sample. For the analysis of the thermal effusivity of agar–titania samples, the process will be considered as a whole process conforming to only a single sigmoidal process. The characteristic times t_0, where the processes reach their maximum velocity are 2000 s for pH 7 and 4000 s for pH 7.5, showing that the increase in alkalinity slows down the dehydration process. This behavior is also observed for the settle-down times, 465 s at pH 7.5 and 193 s at pH 7.

In relation to the fact that these curves show initially a stationary behavior during a well-defined period of time, this response is related to the thermal diffusion length of the different samples. Given that the samples contain a significant quantity of water at the beginning of the process, it can be considered that the effective thermal diffusivity of the samples is near $\alpha \approx 0.0015\,\mathrm{cm}^2\cdot\mathrm{s}^{-1}$ [9]. At the modulation frequency of 7 Hz, the thermal diffusion length would be about $\mu = 80\mu$m. As a consequence of this, using our approach, it is only possible to analyze the process occurring at this length. The observed differences in the initial time are therefore due to factors related to the thermal diffusivity of the samples, but will also be strongly influenced by the dehydration rate.

Sol–gel processes are carried out in two steps: hydrolysis and condensation reactions, which can proceed simultaneously [13, 14]. In the hydrolysis reaction, a metal alkoxide molecule substitutes an hydroxyl group from the water molecule and forms an alcohol. These hydrolyzed species can undergo further hydrolysis, or can interact with another similar species or with another water molecule, to form oxygen bridges between metal atoms. Controlled thermal treatment of the gels provided the final oxide form of the material by a dehydroxylation process.

From the sigmoidal fits for the initial dehydration stages, it can be seen that the values of Δt are higher for pH 7 than for pH 7.5. Meanwhile, this behavior is reversed when the dehydration continues, as can be observed for the Δt_p values in Table I and for the settle-down times for the thermal effusivity. From these results it seems the titania–agar sample with a pH of 7.5 has a behavior that resembles that of the pure titania sample with nearly the same settle-down times. Nevertheless, the total time of the dehydration process of the sample with a pH of 7.5 is the longest.

Since the gellation process of titanium alkoxide is the same at pH 7 and 7.5 [14], the differences in the final stage of the dehydration process must be caused by a modification of the hydrophilic properties of agar. These effects deserve further study in order to understand the hydration process of agar occluded in a ceramic matrix.

Agar is a mixture of polysaccharides, in particular, it is composed of agarose which has an alternate of 3,6-anhydro-L-galactose (3,6 AG)

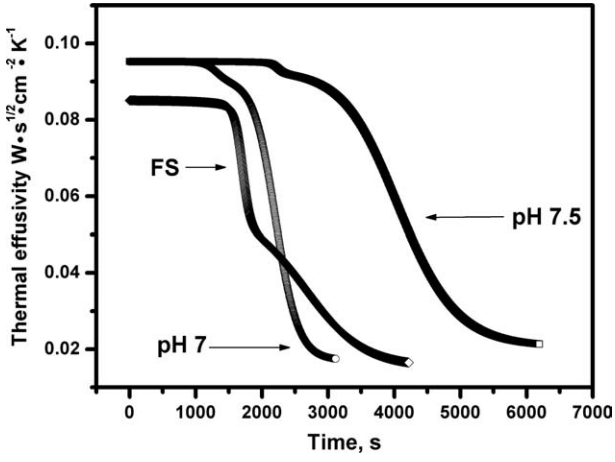

Fig. 3. Calculated thermal effusivity as a function of time for different pH values and for the titania sol–gel matrix without encapsulated agar.

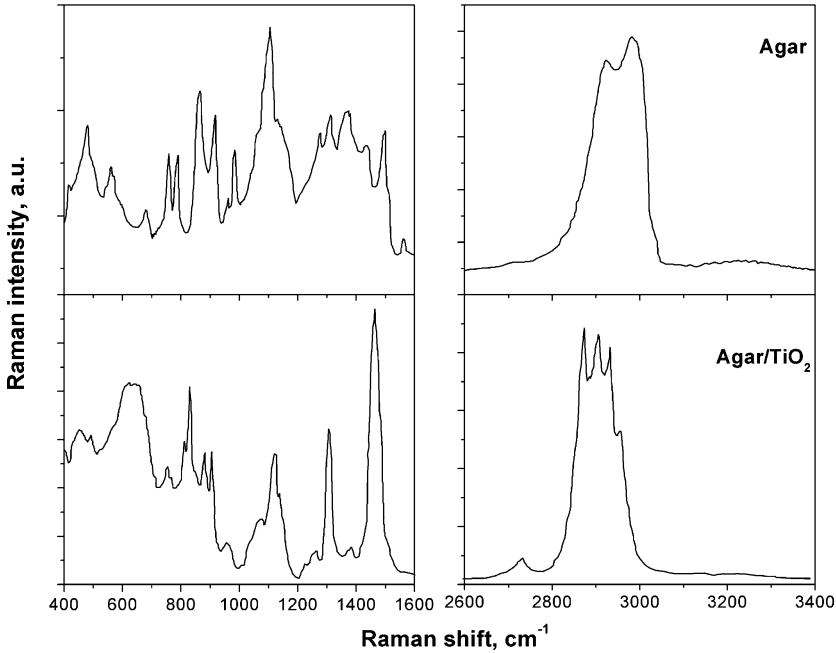

Fig. 4. Raman spectra of agar and agar/TiO_2 at room temperature between 400 and 1600 cm^{-1} and between 2600 and 3400 cm^{-1}.

and D-galactose. From previous studies it has been shown that it contains nearly 41% of 3,6 AG and 2% of sulfate [12]. Raman and FT-IR spectra of pure agar and encapsulated agar are presented at constant pH and room temperature in Figs. 4 and 5, respectively. As can be observed, Raman and absorption spectra are complex with many overlapping bands.

From the absorption spectrum of pure agar, we can observe a broad band centered around 600 cm^{-1} attributed to the liberation mode of residual water molecules [15]; an intense band between 800 and 1200 cm^{-1} corresponding to C−O stretching vibrations, in particular, the absorptions at 890, 934, and 1162 cm^{-1} (ν_{C-O-C}) are assigned to vibrations of the glycosidic linkage [15]; a broad band between 1350 and 1500 cm^{-1} with three maxima at 1384, 1423, and 1467 cm^{-1} due to δ_{CH_2} vibrations; an intense band at 1648 cm^{-1} with a shoulder at 1671 cm^{-1} that can be due to δ_{H-O-H} and $\delta_{C=C}$ vibrations, respectively, but which is probably perturbed by δ_{COCH_3} groups absorption [16]; a broad band centered at 2926 cm^{-1} due to asymmetrical and symmetrical ν_{CH}, and a broad and intense band

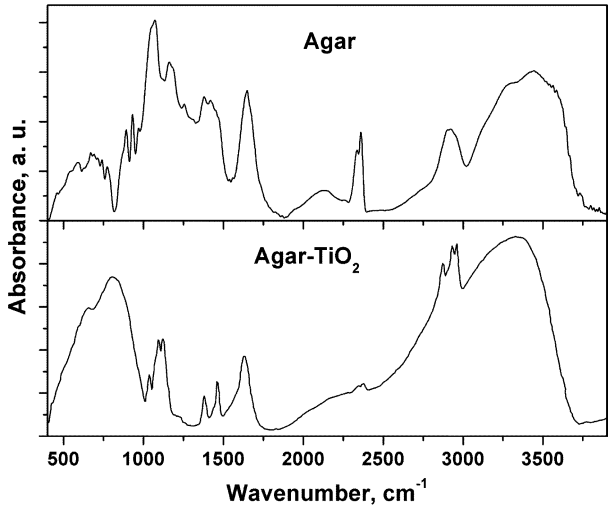

Fig. 5. FT-IR absorption spectrum, between 450 and 3650 cm^{-1}, of agar and agar/TiO_2 at room temperature.

due to ν_{OH} with maxima at 3288, 3442, and 3577 cm^{-1} suggesting that the hydroxyl groups and residual water molecules are hydrogen bonded.

In the Raman spectrum of pure agar (Fig. 4), the bands are generally less broad than in the FT-IR spectrum. From this spectrum, we can observe an intense band in the high frequency region with vibrations at 2914, 2977, and a shoulder at 2954 cm^{-1}, which are the $\nu_s(CH_2)$, $\nu(CH)$, and $\nu_{as}(CH_2)$, respectively [17]; a broad band between 1200 and 1500 cm^{-1} with vibrations at 1495 (δ_{CH_2}), 1375 (ω_{CH_2}), and 1276 cm^{-1} (τ_{CH_2}); an intense band centered at 1104 cm^{-1} (δ_{COH}) with shoulders at 1141 and 1077 cm^{-1} due to sugar and exocyclic ν_{C-O} vibrations, respectively [17,18]; and some sharp bands between 400 and 1000 cm^{-1} at 987 (δ_{CCH}), 915 (δ_{CCH}), 864 (δ_{CC}), 781 (δ_{CC}), 567 (δ_{CCC}), and 480 cm^{-1} (δ_{CCC}). It seems that the multiplicity of bands could be due to the presence of α and β-anomers [19].

When the agar is occluded in TiO_2, the main groups of vibrations are still observed; nevertheless, the intense Raman bands (Fig. 4) of the residual *n*-butoxide are also observed, particularly in the CH stretching (bands at 2880 and 2913 cm^{-1}) and the CH deformation (1450 cm^{-1}) regions, which partly mask the agar spectrum. Some bands due to the agar can be observed at 1380 (ω_{CH_2}), 960 (δ_{CCH}), and between 750 and 900 cm^{-1}. The two vibrations at 449 and 630 cm^{-1} are due to TiO_2 in the anatase phase [20]. The small changes in the frequency of some

bands could result from the interaction between the TiO_2 matrix and the agar.

For the FT-IR spectrum of agar–TiO_2 (Fig. 5), a broad and intense band can be observed due to ν_{OH} vibrations centered at 3342 cm^{-1}, indicating also the presence of OH groups from water, butoxide residues, and agar. This band is correlated to the bands observed near 1633 (δ_{OH}), 1467 (δ_{CH_2}), and 1383 cm^{-1} (ω_{CH_2}). Nevertheless, these last two bands are also present in the absorption spectrum of pure agar. The bands observed at 890, 934, and 1162 cm^{-1} (ν_{C-O-C}) in pure agar seem to shift to 814 and 1124 cm^{-1} in the agar-TiO_2 sample indicating a strong interaction with OH groups. This behavior implies a high hydrophilicity between the agar and the TiO_2 matrix, as previously seen.

4. CONCLUSIONS

The thermal effusivity of the dehydration process of emulsions of encapsulated agar in a titania sol–gel ceramic matrix has been studied. Measurements were performed using conventional photoacoustic techniques. It has been shown that this methodology is strongly sensitive in the analysis of different dehydration processes occurring in the samples. In particular, it has been shown that an increase in pH during the preparation process strongly influences the dehydration rates, as well as settle-down time intervals. These results suggest a strong interaction and hydrophilicity between agar and the titania matrix, which is an important factor to evaluate the usefulness of these materials in the encapsulation of microorganisms.

ACKNOWLEDGMENTS

The authors wish to thank J. Bante and F. Kantun for technical assistance. This work was partially supported by Conacyt Project No. 38493-U.

REFERENCES

1. C. Roux, J. Livage, K. Farhati, and L. Monjour, *J. Sol–Gel Sci. Technol*. **8**:663 (1997).
2. E. Pope, K. Braun, and C. Peterson, *J. Sol–Gel Sci. Technol*. **8**:635 (1997).
3. R. Bhatia, C. Brinker, A. Gupta, and A. Singh, *Chem. Mater*. **12**:2434 (2000).
4. L. Inama, S. Dire, and G. Carturan, *J. Biotechnol.* **30**:197 (1993).
5. G. Kuncova and M. Sivel, *J. Sol–Gel Sci. Technol.* **8**:667 (1997).
6. L. Zheng, K. Flora, and D. Brennan, *Chem. Mater.* **10**:3974 (1998).
7. S. Fennouh, S. Guyon, J. Livage, and C. Roux, *J. Sol–Gel Sci. Technol*. **19**:647 (2000).
8. J. A. Wang, O. Novaro, X. Bokhimi, T. López, R. Gómez, J. Navarrete, M. E. Llanos, and E. López-Salinas, *J. Phys. Chem.* B **38**:7448 (1997).

9. A. Rosencwaig, *Photoacoustics and Photoacoustic Spectroscopy* (Robert E. Krieger, Malabar, FL, 1990), pp. 93–124.
10. M. Vargas-Luna, G. Gutierrez-Juarez, J. R. Rodríguez-Vizcaino, J. B. Varela-Najera, J. M. Rodríguez-Palencia, J. Bernal-Alvarado, M. Sosa, and J. J. Alvarado-Gil, *J. Phys. D: Appl. Phys*. **35**:1532 (2002).
11. L. C. M. Miranda and N. Cella, *Phys. Rev. B* **47**:3896 (1993).
12. Y. Freile-Pelegrin, *J. Appl. Phycol.* **12**:153 (2000).
13. C. J. Brinker and G.W. Scherer, *Sol–Gel Science* (Academic Press, San Diego, 1989), pp. 22–31.
14. R. D. González, T. López, and R. Gómez, *Catal. Today* **35**:293 (1997).
15. K. Haxaire, Y. Maréchal, M. Milas, and M. Rinaudo, *Biopolymers* **72**:10 (2003).
16. A. T. Tu, *Raman Spectroscopy in Biology* (John Wiley, New York, 1982), pp. 234–255.
17. M. Mathlouthi and D. V. Luu, *Carbohydr. Res*. **78**:225 (1980).
18. J. J. Cael, J. J. Koenig, and J. Blackwell, *Carbohydr. Res.* **29**:123 (1973).
19. M. Mathlouthi and D. V. Luu, *Carbohydr. Res*. **81**:203 (1980).
20. M. Picquart, L. Escobar-Alarcón, E. Torres, T. López, and E. Haro-Poniatowski, *J. Mater. Sci.* **37**:3241 (2002).